Research Article

Micro Visual Investigation of Enhanced Oil Recovery in Heterogeneous Pore Network of a Micro Model Using Hybrid Nano Fluid

Amir Hosseinzadeh Helaleh[1*], Mostafa Alizadeh[2], Mohammad Samipoor Giri[3]

[1]Department of Earth Science, University of Barcelona, Barcelona, Spain;[2]Department of Chemical Engineering, Tarbiat Modares University, Tehran, Iran;[3]Department of Chemical Engineering, North Tehran Branch, Islamic Azad University, Tehran, Iran

ABSTRACT

Emerging nanotechnologies, such as nanofluids composed of liquid suspensions of nanoparticles, may soon allow for the accelerated recovery of hydrocarbons and stimulation fluids from oil and gas reservoirs. Nanofluids in Enhanced Oil Recovery (EOR) as a tertiary process employs nanoparticles to reduce the residual oil saturation of the reservoir mainly through Interfacial Tension (IFT) reduction and wettability alteration. In spite of its great potential and the mentioned advantages, application of nanofluids in EOR has been limited because of the lack of practical convincing experimental results. In this study, the effects of hybrid nanofluid in EOR process on wettability and IFT changes and the reduction of residual oil saturation have been examined by providing microscopic visualization of two phase flow in transparent glass micromodels TiO_2-Cu nanoparticles were used to investigate its impacts on wettability of the micromodel pore walls by measuring the relative permeabilities before and after treatment. Results indicated that wettability of the pores was altered towards more water wetness which was also supported by visual observation of the oil/water phase saturations in the glass micromodel. Moreover, the oil recovery was increased up to 245% of the Original Oil In Place (OOIP) during the EOR process.

Keywords: Micro model; Oil recovery; Nano composite; Hybrid nano fluid

INTRODUCTION

With increased demand for oil, more countries and companies are evaluating and applying enhanced oil recovery techniques to achieve the full potential of producing assets. EOR means oil recovery beyond the usual primary and secondary stages EOR application depends on the oil properties and reservoir characteristics. Several different EOR technologies have emerged during; the last decades in order to optimize oil recovery after conventional recovery methods have been applied Much work has been performed in the area of fluid injection with the objective of improving oil recovery by the natural drive mechanism EOR techniques will contribute to a longer life time of already existing reservoirs Unfortunately the application of EOR does not only bring advantages. Using EOR is correlated with higher risks and increases the requirement for additional facilities and investments.

The three major types of enhanced oil recovery operations are chemical flooding (polymer, surfactant or alkaline floods), miscible displacement (carbon dioxide [CO_2] injection or hydrocarbon injection), and thermal recovery (steam flood or in-situ combustion). The optimal application of each type depends on reservoir temperature, pressure, depth, net pay, permeability, residual oil and water saturations, porosity and fluid properties such as oil density and viscosity.

Chemical methods of enhanced oil recovery became widely popular during the 1980s [1]. Chemical methods aim to increase the amount of oil recovered by either increasing the effectiveness of water floods by modifying the water used to displace the oil, by reducing the interfacial tension between the imbibing fluid and the oil with the use of a host of different surfactants, or by modifying the wettability of the oil fields substrate to make it lyophobic [1-4]. Chemical methods use either alkali-polymers, surfactant polymers, or more recently a combination alkali-surfactant polymer system [2]. The larger challenge with chemical methods is that every possible variable with respect to fluid and substrate properties can change from one oil reservoir to the next and thus the chemistry must be tailored specifically for any given reservoir. There is a large body of work for conditions in and solutions to enhanced oil recovery in

particular oil fields, summarized in a few works [2,5,6].

The main challenge resulting from the use of surfactants to lower the interfacial tension or polymers as a thickener is its delicate relationships to the conditions of the oil field substrate, which is not always constant, and the oil properties, which can also vary. Oftentimes, the polymers or surfactants are applied too far into the initial water flood, or they can lose effectiveness midway through the field [7]. Another challenge with chemical approaches to enhanced oil recovery is cost; depending on the fluctuating cost of oil and production, it can quickly become the prohibiting factor. While challenging, the vast amount of oil remaining within oil fields is only going to be a growing driving factor for EOR research as the easilyaccessed oil is recovered and consumed.

Recently, the oil industry has been approaching nanotechnologies as a potential solution to the abovementioned challenges, calling for the same breakthrough effects that this relatively new branch of science has been gushing over the last 20 years in aerospace, biology and medicine [8-12]. Properties of Nano materials such as lightness, corrosion resistance and mechanical strength are and will be significant enablers, for example, for drilling and completion activities. Nanotechnology could also represent a breakthrough element for prospection, thanks to the development of innovative monitoring techniques and smarter micro/nano sensors. Other emerging applications of nanotechnology are represented by the development of new types of "smart fluids" for water shut-off and improved/enhance oil recovery [13].

These nano agents can drastically increase oil recovery by improving the geo mechanics of a reservoir through the improvement of surface tension as well as actual modification of the reserves themselves. The viscosity of a fluid injected to displace oil, such as water, CO_2 or surfactant solution, is often lower than the viscosity of the oil In this situation, adding nano particles can tune up the viscosity of the injected fluid to an optimum level, with net effect of improving the mobility, thus the oil recovery efficiency. Several studies have reported that upon addition of the nanoparticles, the properties of the base fluid such as density, viscosity, thermal conductivity and specific heat can be increased [14-19].

In the present work, Al2O3-Cu nano composite powder has been synthesized by a thermochemical method Al2O3-Cu/brine hybrid nano fluids were then prepared by dispersing the synthesized nano composites powder in brine solution. The objective of the present experimental investigation is to contribute to the rare hybrid nano fluid implementation in enhance oil recovery process. Experiments were conducted in a micro model which had geometrically and topologically the same homogenous pore space as Berea sandstone. It acts as an artificial reservoir and is an etched silicon wafer bonded with glass to build the flow channels. The main advantage compared to conventional core experiments is that the displacement process can be observed at macro and micro scale with a microscope without any CT-scanning tools Records in form of high resolution photographs and videos describe the displacement process at micro and macro scale Finally, IFT and contact angle (θ) are parameters which were evaluated in this study.

METHODOLOGY

Fluids

Degassed crude oil from a field in Ahwaz-Iran was used as the oleic phase in this study. This oil has a viscosity of approximately 52 cP at 25°C. For the base aqueous phase, synthetic reservoir brine was prepared from sodium chloride (NaCl) at 30 wt % (approx 30,000 ppm) and deionized water. The density and viscosity were measured using a pycnometer and a Brookfield rotating viscometer, respectively. The pH and surface conductivity were measured using a digital pH meter Metro ohm (serial 827). This brine was used as the dispersion fluid for the NPs, and the fluid properties are summarized in Table 1. Adding NPs into the brine slightly decreased its density and pH value, whereas the viscosity and surface conductivity were increased.

Table 1: Fluid properties measured by using digital pH meter in nano fluid solution.

Fluid	Density (g/cm³)	Viscosity(cP)	pH
Oil	820	5.2	-
Brine	1.02	1.001	6.6
Nanofluid	1.027	1.1	6.3

Nanoparticle preparation and characterization

The facile preparation of the copper-titania hybrid nano composite (HyNC) consisted of the following steps :(1) ultrasonic dispersion of an aqueous solution containing titania (5 g). (2) intense stirring and mixing of a copper acetate (05 g) aqueous solution, containing ascorbic acid and sodium borohydride reducing agents with the prepared titania aqueous solution, for 2 h at 45oC and ambient pressure, for subsequent production of HyNC colloids.(3) washing and filtration of the HyNC colloids followed by vacuum drying. (4) Ultrasonic re-dispersion of the as-prepared HyNC powder into the base fluid, in volume concentrations ranging from 01% to 20% using the ultrasonic vibrator (UP200S-Hielscher).

The surface morphology of the Cu-TiO$_2$ nano composite was examined by a high resolution field emission scanning electron microscope (FESEM: SUPRA55, Carl Zeiss, Germany, Electron High Tension (EHT): 20 kV) which shows that the as-prepared particles are in the form of tiny agglomerates and nearly spherical in shape (Figure 1). The composition of the Cu-TiO$_2$ nano composite was measured by the EDAX analysis, and the crystallite size and structure of the CuTiO$_2$ nano composite was measured by the XRD analysis characterization techniques, as shown in Figures 2a and 2b. The average grain size of the hybrid particles was calculated to be 17 nm using Scherrer formula.
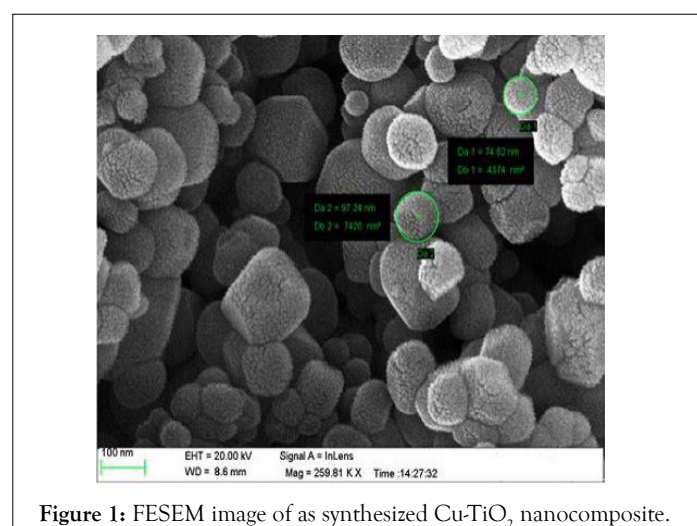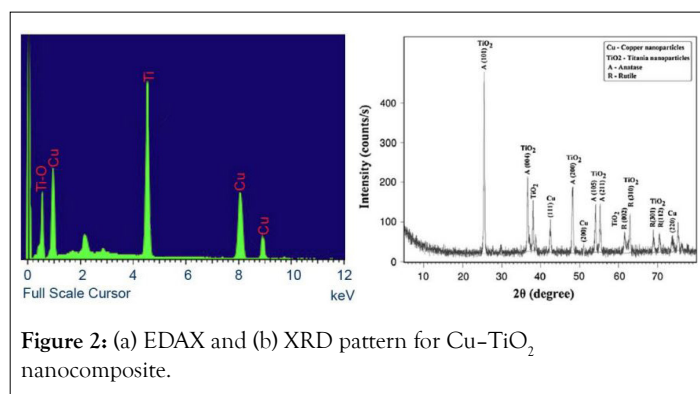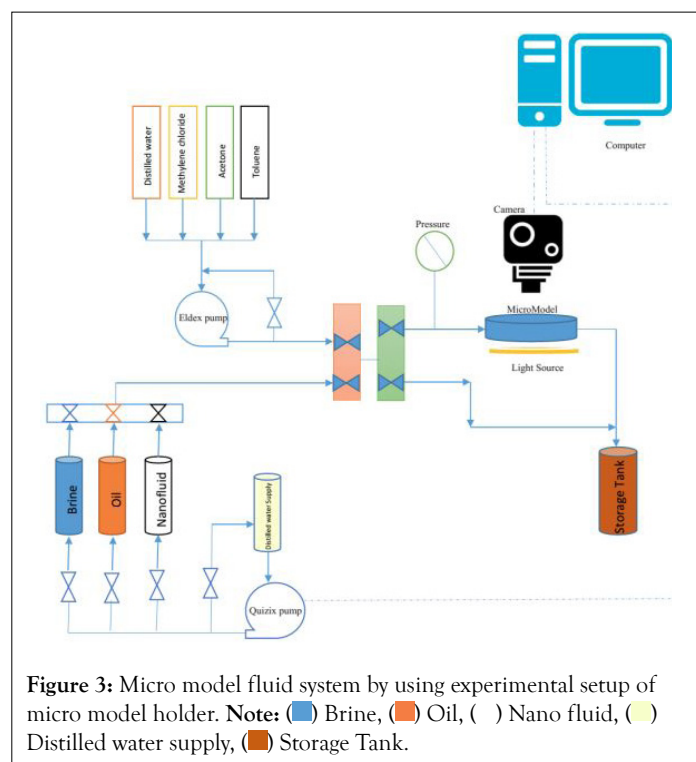

Figure 1: FESEM image of as synthesized Cu-TiO$_2$ nanocomposite.

Figure 2: (a) EDAX and (b) XRD pattern for Cu–TiO$_2$ nanocomposite.

The as-prepared Cu-TiO$_2$ nano composite was re-dispersed in brine using UP200S-Hielscher ultrasonicator, to prevent uncontrolled agglomeration of powders due to intermolecular forces of attraction. A polyvinyl pyrrolidone (PVP: C6H9NO) stabiliser known as Povidone is used in this study. This material has an ultrafine amorphous form, a size of approximately 50-250 lm and a bulk density of 400-600 g/L. The advantage of PVP is its universal solubility both in hydrophilic and hydrophobic solvents, and it is a non-toxic stabiliser that is safe for the environment. Currently, PVP is widely used as a binder for capsules and granules (especially in pharmaceuticals), a film former in medical plastics, a taste masker in chewable tablets and a toxicity reducer. In this study, PVP type K30 was added to avoid earlier NP aggregation by improving the metal oxide nanofluid stability. The K30 refers to the K value of this PVP in the range 270-324. The K value characterises the mean molecular weight of PVP, and the higher the K values, the higher the molecular weight.

Micromodel

The micromodel setup was composed of four parts including cleaning system, fluid injection section, optical system, and micromodel holder. Figure 3 shows a schematic diagram of the experimental setup. Cleaning was accomplished by flushing solvent through micromodel using an Eldex pump. This pump was connected to four containers that contained cleaning fluids (ie, distilled water, methylene chloride, acetone, and toluene). A precise pressure transducer and a high-accuracy low-flow-rate. Quizix pump were used to control the injection flow rate of fluids. The Quizix pump was able to inject at rates varying from 10^{-5} to 10 cm^3 min^{-1}. A Rosemount 3051 Differential Pressure transmitter (DP) (with 004% span reference accuracy and capability of measuring differential pressures between 0 and 2000 psia) is placed to the line connected to the micromodel inlet port to measure pressure drop in the micromodel during the tests. Micromodel was held above a LED light box to remove shadow effects and increase the quality of captured pictures. In this study, the visual data acquisition was achieved by using high-resolution optical equipment for image capturing and analysis. A computer-controlled linear drive system was used which allowed a magnifying video camera to be positioned automatically at any part of the micromodel and sequentially or continuously record the phase displacements occurring within the micromodel. The camera was capable of working at a magnification up to 200 times. While running the experiments, in addition to continuous video recording, pictures of micromodel were digitally captured and recorded by a computer. The pictures were later used for image analysis and saturation measurement purposes.

Figure 3: Micro model fluid system by using experimental setup of micro model holder. **Note:** (■) Brine, (■) Oil, ( ) Nano fluid, ( ) Distilled water supply, (■) Storage Tank.

To analyze the experiments' results, it was necessary to measure fluid saturation variations within micromodel Sigma Scan Pro 50 image analysis software and statistical analyses were used to obtain detailed characterization of porous medium and measurement of the fluid saturations from the micromodel micro shots. Sigma Scan is capable of counting the number of pixels having a specific color (ie, connate-water: blue, oil: brown, nano fluid: white). More precisely, the saturation of each phase was obtained by dividing the number of its pixels by the total number of pixels from all phases. The oil recovery at any injected pore volume is equal to the areal weep efficiency The oil recovery or areal sweep efficiency is calculated from the following relation:

EA=(Soi-Sor)/Soi   (1)

Where EA is a real sweep efficiency and Soi and Sor is initial and remaining oil saturation, respectively.

Preparation of micromodel

Although conventional glass micro-models were extensively used for laboratory EOR experiments, they suffer from some shortcomings, such as time consuming, high expenses, safety, and difficulty to control pore geometrical characteristics during model construction. In this work, a CO$_2$ laser device was used to construct flow patterns on the glass surfaces.

In this work, a quarter five-spot glass micromodel was constructed by laser technique before performing the flooding tests [20]. The following steps have been performed in the experiments to construct the models.

Drawing patterns: In this part, Corel-Draw and Auto-Cad software were used to draw the mask of patterns. Different types of patterns, including a desirable network of pores and throats as well as rock-look-alike patterns generated from a thin section of reservoir rock can be prepared by this software. Figure 4 shows pattern used in the micromodel.
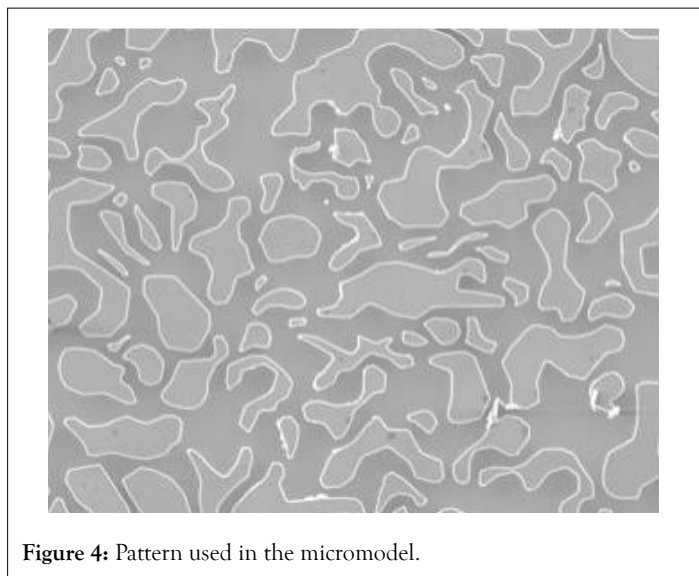
Figure 4: Pattern used in the micromodel.

Laser process : After planning the pattern by graphical software, to construct a model with controlled pore morphology and heterogeneity, the laser parameters should be adjusted. The CO_2 laser device with power of 120 W was used to etching and constructing glass micromodel in siliceous glasses with dimension of 20 cm × 15 cm × 6 mm.

Fusing process: After the preparation of the pattern, a second, optically flat, glass plate was placed over the first, covering the etched pattern and, thus, creating an enclosed pore space. This second plate, the cover plate, had an inlet hole and an outlet hole drilled at either end, allowing fluids to be displaced through the network of pores. This combination was placed into a special oven with its temperature and heat flux controlled automatically. The heating process started from ambient temperature to 745°C gradually. After this, the oven is left to cool down slowly this heating process, named the fussing process, was performed in order to completely seal the micro-model and to provide an overburden pressure during the entire experiment.

Figure 5 shows a close-up view of scanning electron microscope image. This pattern was prepared by thin section of carbonate rock from one of Iranian oil reservoir. The micromodel constructed by laser method can acceptably demonstrate the surface heterogeneity and roughness of the porous media. The rough surface is demonstrated in Figure 5.
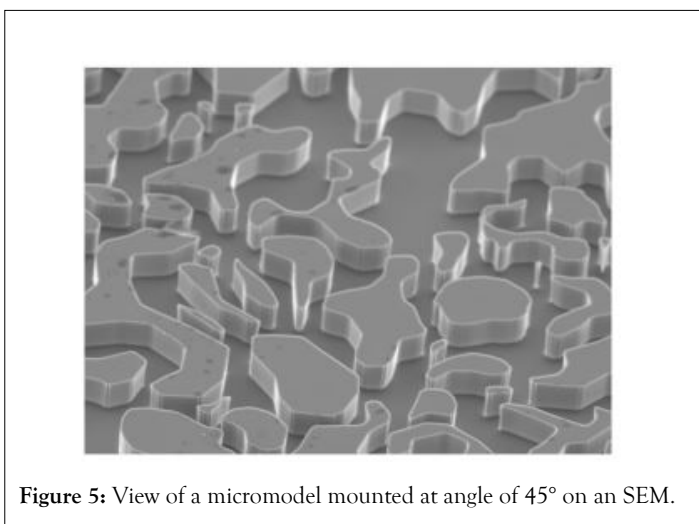

Figure 5: View of a micromodel mounted at angle of 45° on an SEM.

When the micromodel was built, its physical and hydraulic properties were determined either by using image analysis or experimental measurement. The average etched depth was measured by using Mitutoyo (NO3109F) depth measurement apparatus. The image analysis was used to estimate the areal porosity of the micromodel after it was filled with colored water. The pore volume of the micromodel was calculated using its areal dimensions and average etched depth Absolute permeabilities of micromodel were measured by conducting one-dimensional flow experiments, and using Darcy's law by recording pressure drops at numerous different flow rates. To determine the absolute permeabilities, for which one-dimensional Darcy flow condition is required, one-dimensional micromodels with length of 60 mm and width of 10 mm were prepared the one dimensional micromodels had same pore structure, pore network, and average etching depth of the two-dimensional micromodels. Based on the similarity of physical properties, it was assumed that absolute permeabilities of two-dimensional micromodels are the same as the calculated permeabilities of one-dimensional micromodels. Each determination test was repeated to examine the accuracy of the results. The physical properties of the two-dimensional micromodels are given in Table 2.

Table 2: Distribution of pore-body and pore-neck size of micromodel in core properties.

Dimension (cm²)	Average etched depth (mm)	Coordination number	Porosity (%)	Absolute permeability (D)
20 × 10	0.065	3	36	1.6

It is worth noting that coordination number is number of pore-necks that connected to a pore-body. Moreover, the frequency distribution of pore-body and pore-neck size of micromodel is shown in Figure 6.
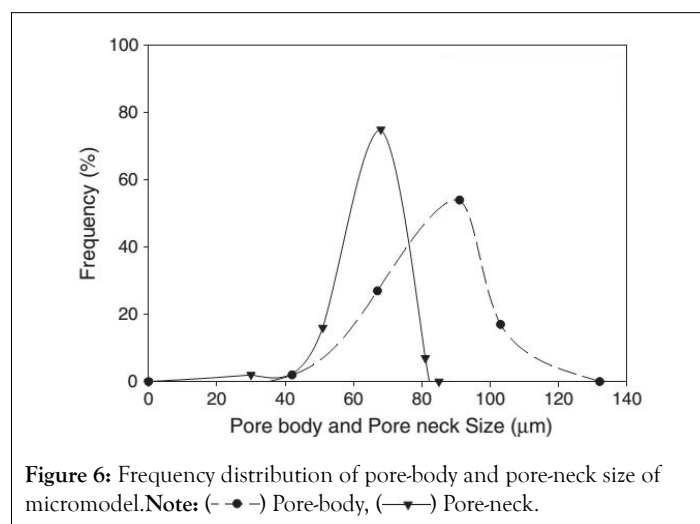

Figure 6: Frequency distribution of pore-body and pore-neck size of micromodel. **Note:** (– ● –) Pore-body, (—▼—) Pore-neck.

Procedure to make an oil-wet medium

The general procedure for altering the wettability of micromodels to oil-wet is as follows: (1) Soak the micromodel thoroughly in sodium hydroxide for one hour. (2) Rinse the micromodel thoroughly with distilled water to remove all residues, and then dry using an oven set on 200°C for at least 15 min. (3) Saturate the micromodel with the solution of 2% Tri Chloro Methyl Silane (TCMS) in dehydrate toluene for at least 5 min, a thin film immediately coats micromodel's internal surface, making it water repellent. (4) Rinse the micromodel with methanol to remove excess siliconizing fluid.

(5) Dry the micromodel using an oven set on 100°C for 1 h to cure the silicone coating.

Permeability measurement

To confirm wettability alteration through relative permeability measurements, the oil and water relative permeabilities must be compared for the two cases, fresh micromodels and nanofluid treated model (after flooding tests).

The relative permeability data with respect to water saturation could be obtained by either steady-state or unsteady-state measurement techniques. Since the application of unsteady state methods needs negligible capillary effects, steady-state method was found to be suitable for measuring relative permeability at capillary flow condition of the micromodel system.

During the steady-state technique, different ratios of brine and oil were injected simultaneously into the model until the steady-state condition of pressure and saturation is established. Pressure drop through the porous medium was measured and water saturation was determined using image processing techniques.

Relative permeabilities are then calculated by direct use of multiphase extension of Darcy's law:

$$k = \frac{-q\mu_w}{A}\frac{L}{\Delta P} \qquad (2)$$

where A is the cross sectional area, ΔP is the pressure drop, μ is the viscosity of water, q is the volumetric flow rate, L is the length, and k is the absolute permeability. Several steady state pressure drops across the micromodel were measured at specific flow rates. Using the dimensions of the micromodel, known constants, and measured variables, the plot (qμwL) versus (A ΔP) was constructed to find a slope that is equal to permeability k.

Finally the washing procedure was applied to the model using alternative injection of ethanol (water phase solvent) and normal heptane (oil solvent), followed by air-drying. Flow rates were then changed in a way that increasing water saturation can be achieved. If other parameters were known, individual injection rates and pressure data could be used to calculate oil and water relative permeabilities according to Equation 2.

Contact angle measurement

The contact angle was measured directly on transparent plates using a Goniometry KSV CAM instrument at ambient conditions.

It is defined the contact angle in a three phase system (water, oil and rock surface) as follows: water-wet in the range of 0°-75°, intermediate/neutral-wet in the range of 75°-105° and oil-wet in the range of 105°-180°. A zero contact angle indicates that the denser fluid completely wets the solid.

Interfacial tension measurement

The Interfacial Tension (IFT) of degassed crude oil was measured against brine/nanofluid as the aqueous phase using a SVT20 spinning drop video tensiometer at room temperature. This measurement involves crude oil with brine and nanofluid.
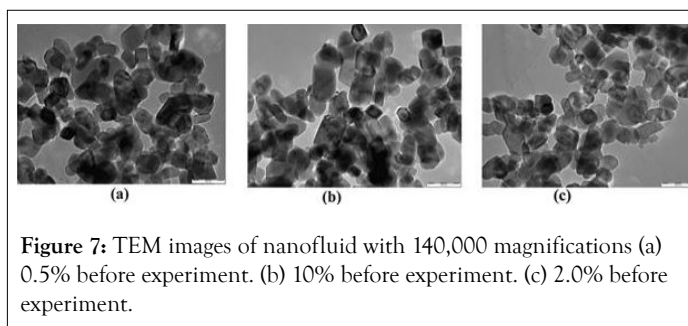
RESULTS AND DISCUSSION

Nanofluid stability

Providing a stable nanofluid is challenging, because NPs have a tendency to aggregate due to forces of different natures that interact amongst particles and may lead to agglomeration. Decreasing the stability of nanofluids will reduce their advantages. The stability of nanofluids is a function of its concentration as dispersed in brine During the injection process, the tendency of NPs to agglomerate will affect the porosity and impair permeability.

The measurement of pH, electrical conductivity and images from Transmission Electron Microscopy (TEM) were undertaken in order to determine the condition of nanofluid agglomeration, dispersion and stability. The stability of nanofluid is strongly influenced by the pH value. The initial pH value of procured nanofluid is 65 which are approximately neutral in nature. The size, shape and stability of the nanoparticles can be observed from the TEM photographs presented as Figures 2a and 2b taken before the conduct of experiment for three different concentrations. The particle size varies between 30 and 50 nm. The surface area of the nanoparticles from TEM images is used to determine the average size of the particle. The cross sectional area of nanoparticle was also determined using Image Processing and Analysis in Java (Image J) software. The average size of nanoparticle suspension in brine is determined to be 50 nm. The shape of the particles is non-spherical and the particles are dispersed without agglomeration. To further establish the stability, the electrical conductivity of a sample nanofluid is determined. The stability of nanofluid depends critically on the surface charge of nanoparticles which is related to electrical conductivity. The value of electrical conductivity is measured before and after the conduct of experiment. A good agreement of the values can be observed from Figure 7 confirming the stability of the nanofluid. The surface conductivity is inversely related to the pH value, and the higher the particle charge potential, the more stable is the nanofluid. The surface conductivity is closely related to the surface charge. If the charge is sufficiently high, the colloids will remain discrete and dispersed in suspension.

Figure 7: TEM images of nanofluid with 140,000 magnifications (a) 0.5% before experiment. (b) 10% before experiment. (c) 2.0% before experiment.

One of the main reasons for using NPs for EOR purposes is to deliberately change the wettability. The wettability alteration occurs if NPs are adsorbed on the surfaces of the grains. Therefore, NPs transportation tests should be performed prior to the NPs being applied for EOR purposes in order to determine the amount of NPs adsorption on the rocks' surfaces Particle straining and adsorption on the grain surface are the two main factors which govern colloidal particle transport through a porous medium. As particles flow through a porous medium, some may be trapped behind subminiature pore throats, known as "straining". Filtration is defined as irreversible adsorption of the particles onto the porous medium grain surface as a result of attractive interactions between particles and the grain surface. Straining during NPs transportation is not common since the size of the NPs is much smaller than the pore throat dimensions. Therefore, NPs transportation tests were carried out to determine the tendency of the NPs to adsorb on the surface of the limestone due to filtration. The first transportation

test was performed to study nanofluid on the limestone porous medium. The NPs appeared in the outlet right after 1 PV of injection.

The NPs concentration in the effluent then noticeably increased until 15 PVs. Thereafter, the trend showed a moderate decrease until 275 PVs. Above this PV, was not observed in the effluent, even after addition of an extra 10 PVs of DIW. The final results show that 918% of injected Cu/TiO_2 has been recovered. As a result, low-affinity adsorption on the limestone is attributed to Cu/TiO_2NPs. The main reason is the electric surface charges of the Cu/TiO_2NPs and limestone grains, which are both positive (Figure 8).
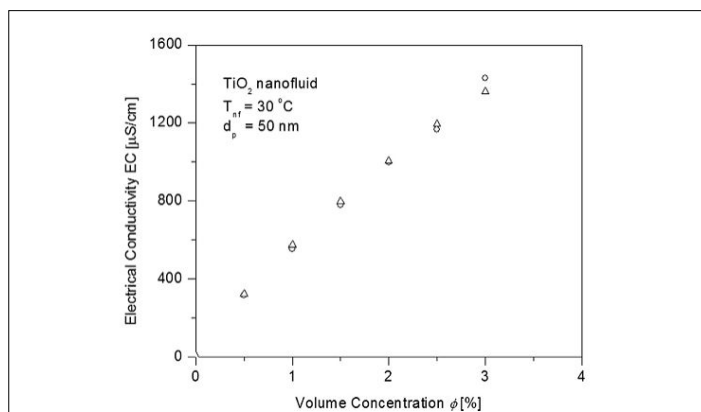

Figure 8: Electrical conductivity of TiO_2/Cu-brine nanofluid at 30ºC. **Note:** (O) Before experiment, (Δ) After experiment.

Microscopic observations

Qualitative investigation of the effect of nanofluid on system wettability was made through comparison between microscopic images before the nanofluid flooding. These images have been presented as follows:

Microscopic images of the fresh models showed a continuous oil phase and individual water drops flowing at the center of the pores which indicate the initial oil-wet condition (Figure 9a).
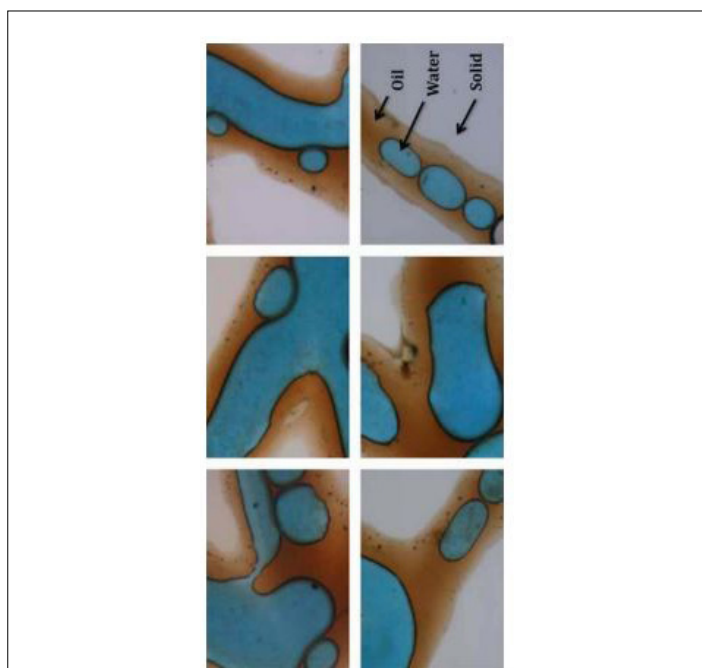

Figure 9a: Oil layer has almost replaced with water phase in some parts of pore walls.

After treatment with nanofluid with 1% nanoparticle concentration as illustrated in Figure 9b, oil layer has almost replaced with water phase in some parts of pore walls. Also, oil phase was moved mainly to the center of pores which is considered as another sign of shifting toward more water-wetness.
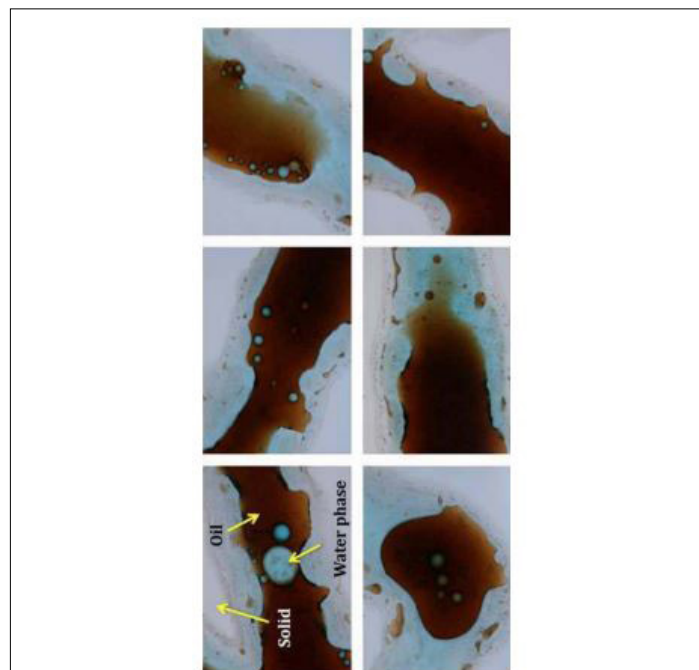

Figure 9b: The effect of nanoparticles with concentration of 2% on two-phase flow distribution.

The effect of nanoparticles with concentration of 2% on two-phase flow distribution was investigated. Oil film covers the surfaces of the pores in many regions of the pore surfaces indicating insignificant wettability change. Moreover, considerable amounts of macro-emulsions have been representative of a noticeable reduction in oil-water interfacial tension.

A comparison between the images captured in these tests showed that wettability alteration efficiency due to nanoparticle treatment was much more effective when bacterial cells were present in the solution.

Analysis of the configuration of the flow pattern at different wettability and pore morphologies would help in understanding of the effects of these parameters on the macroscopic displacement behavior Figure 10 shows the configuration of the flow pattern at different flooding at breakthrough of injected fluid.

When polymer solution moved about half way through the micromodel, it started to finger toward the outlet, which was the low pressure point of the model In the case of oil-wet medium polymer solution fingering started from the injection point and a stable polymer solution front did not occur. This is due to the effects of wettability which caused the formation of thin streams of polymer solution. The mixed-wet medium showed relatively good stable front and also polymer solution completely swept some part of the medium.

In the case of water-wet medium, polymer solution formed a wide and stable front which resulted in high sweep efficiency (Figure 10a). In the mixed-wet medium, polymer solution swept more wetted areas (Figure 10b). Although polymer solution spread non-uniformly over most parts of the micromodel, polymer flood performance was not as good as in the water-wet medium. Figure 10c demonstrates that polymer solution fingered toward the outlet

in the oil-wet medium In general, flow pattern in micromodel B-1 is more uniform and the front is slightly more stable than in micromodel A-1, due to the higher coordination number of the medium.
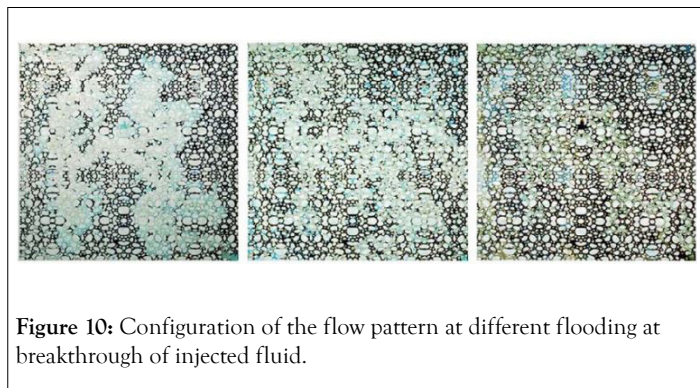

Figure 10: Configuration of the flow pattern at different flooding at breakthrough of injected fluid.

CONCLUSION

In this study, the effects of hybrid nanofluid in EOR process on wettability and IFT changes and the reduction of residual oil saturation have been examined by providing microscopic visualization of two phase flow in transparent glass micromodels. TiO_2-Cu nanoparticles were used to investigate its impacts on wettability of the micromodel pore walls by measuring the relative permeabilities before and after treatment. Results indicated that wettability of the pores was altered towards more water wetness which was also supported by visual observation of the oil/water phase saturations in the glass micromodel. Moreover, the oil recovery was increased up to 245% of the Original Oil in Place (OOIP) during the EOR process.

REFERENCES

1. Alvarez JM, Sawatzky RP. Waterflooding: Same old, same old? InSPE Heavy Oil Conference-Canada 2013. OnePetro.

2. Kong X, Ohadi MM. Applications of micro and nano technologies in the oil and gas industry-an overview of the recent progress. In Abu Dhabi international petroleum exhibition and conference. OnePetro. 2010,

3. Tabary R, Bazin B, Douarche F, Moreau P, Oukhemanou-Destremaut F. Surfactant flooding in challenging conditions: Towards hard brines and high temperatures. InSPE Middle East Oil and Gas Show and Conference 2013 Mar 10. OnePetro.

4. Levitt, DB; Pope GA. Selection and Screening of Polymers for Enhanced-Oil Recovery.2008.

5. Wu Y, Mahmoudkhani A, Watson P, Fenderson T, Nair M. Development of new polymers with better performance under conditions of high temperature and high salinity. InSPE EOR conference at oil and gas West Asia 2012 Apr 16. OnePetro.

6. Ayatollahi, S.; Ze.rafat, M. M. Nanotechnology-assisted EOR techniques: New solutions to old challenges. SPE 2012

7. Zhang T, Davidson A, Bryant SL, Huh C. Nanoparticle-stabilized emulsions for applications in Enhanced oil recovery. SPE. 2010.

8. Miranda CR, de Lara LS, Tonetto BC. Stability and mobility of functionalized silica nanoparticles for enhanced oil recovery applications. InSPE international oilfield nanotechnology conference and exhibition 2012 Jun 12. OnePetro.

9. Hashemi R, Nassar NN, Pereira Almao P. Enhanced heavy oil recovery by in situ prepared ultradispersed multimetallic nanoparticles: A study of hot fluid flooding for Athabasca bitumen recovery. Energy Fuels. 2013;27(4):2194-201.

10. Ponnapati R, Karazincir O, Dao E, Ng R, Mohanty KK, Krishnamoorti R. Polymer-functionalized nanoparticles for improving waterflood sweep efficiency: Characterization and transport properties. Ind Eng Chem Res. 2011; 50(23):13030-13036.

11. Ju B, Fan T, Ma M. Enhanced oil recovery by flooding with hydrophilic nanoparticles. China Particuology. 2006; 4(1):41-46.

12. Ju B Fan T. Experimental study and mathematical model of nanoparticle transport in porous media. Powder Technol. 2009; 192(2):195-202.

13. Ju B, Dai S, Luan Z, Zhu T, Su X, Qiu X. Study of wettability and permeability change caused by adsorption of nanometer structured polysilicon on the surface of porous media. SPE. 2002.

14. Hendraningrat L, Li S, Torsæter O. September. Effect of some parameters influencing enhanced oil recovery process using silica nanoparticles: An experimental investigation. In SPE Reservoir Characterization and Simulation Conference and Exhibition. OnePetro. 2013

15. Hendraningrat L, Li S Torsaeter O. Enhancing oil recovery of low-permeability Berea sandstone through optimized nanofluids concentration. In SPE enhanced oil recovery conference. OnePetro. 2013

16. Hendraningrat L, Li S, Torsaeter O. A coreflood investigation of nanofluid enhanced oil recovery in low-medium permeability Berea sandstone. In SPE International Symposium on Oilfield Chemistry. OnePetro. 2013

17. Karimi A, Fakhroueian Z, Bahramian A, Pour Khiabani N, Darabad JB, Azin R, et al. Wettability alteration in carbonates using zirconium oxide nanofluids: EOR implications. Energy Fuels. 2012; 26(2):1028-1036.

18. Giraldo J, Benjumea P, Lopera S, Cortés FB, Ruiz MA. Wettability alteration of sandstone cores by alumina-based nanofluids. Energy Fuels. 2013; 27(7):3659-3665.

19. Sun T, Wang G, Feng L, Liu B, Ma Y, Jiang L, et al. Reversible switching between superhydrophilicity and superhydrophobicity. Angew Chem Int Ed. 2004; 43(3):357-360.

20. Shirtcliffe NJ, McHale G, Newton MI, Perry CC, Roach P. Porous materials show superhydrophobic to superhydrophilic switching. ChemComm. 2005; 25(5):3135-3137.